

Two-time scales, two-temperature scenario for nonlinear rheology

Ludovic BERTHIER^{‡,*}, Jean-Louis BARRAT^{*} and Jorge KURCHAN[‡].

[‡]*Laboratoire de Physique*

ENS-Lyon and CNRS, F-69364, Lyon Cedex 07, France

^{*}*Département de Physique des Matériaux*

Université Claude Bernard and CNRS, F-69622 Villeurbanne Cedex, France

(August 13, 2021)

We investigate a general scenario for “glassy” or “jammed” systems driven by an external, non-conservative force, analogous to a shear force in a fluid. In this scenario, the drive results in the suppression of the usual aging process, and the correlation and response functions become time translation invariant. The relaxation time and the response functions are then dependent on the intensity of the drive and on temperature. We investigate this dependence within the framework of a dynamical closure approximation that becomes exact for disordered, fully-connected models. The relaxation time is shown to be a decreasing function of the drive (“shear thinning” effect). The correlation functions below the glass transition temperature (T_c) display a two-time scales relaxation pattern, similar to that observed at equilibrium slightly above T_c . We also study the violation of the fluctuation dissipation relationship in the driven system. This violation is very reminiscent of the one that takes place in a system *aging* below T_c at zero drive. It involves in particular the appearance of a *two-temperature* regime, in the sense of an effective fluctuation dissipation temperature [1]. Although our results are in principle limited to the closure relations that hold for mean-field models, we argue that a number of the salient features are not inherent to the approximation scheme, and may be tested in experiments and simulations.

PACS numbers: 05.70.Ln, 64.70.Pf, 83.50.Gd

LPENSL-TH-18/99

I. INTRODUCTION

The behavior of complex systems subject to an external drive is a very complex field of research. The generic situation we may think of is the case of a fluid undergoing steady shear flow, in which case the study of its response pertains to the field of rheology. Rheological experiments on complex fluids are known to display a rich phenomenology, as illustrated in the recent book by Larson [2]. Non-trivial behaviors, however, are not restricted to complex fluids, since it is also found that supercooled liquids exhibit a non-Newtonian “shear thinning” behavior [3].

From a fundamental and theoretical point of view, the most interesting features emerge when the intrinsic relaxation time scale of the system become of macroscopic order, so that there is a direct interplay between the “shearing” time scale and the relaxation time scale. This means that we will be interested in systems whose dynamical evolution exhibits a *two-time scales* pattern. This is the case e.g. in supercooled liquids, in which the particles have a fast “rattling” motion inside the “cage” constituted by their neighbors, followed by a slow “structural” rearrangement of these cages. The two time scales become more and more different on approaching the glass transition. Below the glass transition the same behavior subsists, but now the time scale of the structural relaxation (the α -relaxation time t_α) is not constant and grows with the waiting time elapsed after the quench to low temperatures: this gradual arrest is called aging. More generally, the same situation is realized in all systems that are “jammed”, like granular materials or foams [4]. In all these cases, it is known that a driving force has a particularly strong influence, for it may be able to stop the aging in an out of equilibrium system and to restore time translation invariance.

In order to study theoretically this interplay between the drive and the relaxation of the system, it is natural to extend the approaches that have been successful for describing the dynamical behavior of glassy systems, as reviewed e.g. in [5]. One possible and quite promising route, followed by Sollich and coworkers (for a review, see [6] and references therein) is to extend the phenomenological “trap” models to driven systems, giving rise to

the so-called SGR model. Such a model was shown to account well for a number of the generic features found in soft glassy materials.

Another possible, and complementary, approach is to extend the mode-coupling approach used in the study of glassy systems to the driven case. This approach relies on a closure relation for the dynamical equations that is known to be exact for “mean-field” like systems, and to provide a reasonably good description of the dynamics of real glass forming liquids [7]. This theoretical framework has the advantage of simultaneously giving insights into the macroscopic (rheological) and the microscopic (non-equilibrium statistical mechanics) aspects of the problem, since the mode-coupling equations can be derived from specific microscopic models.

Such microscopic models with driving forces have been first studied in the context of neural networks [8,9], the drive being a tool to destroy the glassy phase. More closely related to our approach are the studies of Horner [10] and Thalmann [11] who investigated the dynamics of a particle in a random potential in the presence of a driving force. Our focus in this paper will be a bit different, since we are interested in translating the results into the language of non-linear rheology.

The paper is organized as follows. In the next section we explain the general spirit of the closure approximations that give rise to the mode-coupling equations. An explicit example for a simple system is worked out, and the numerical methods used in solving the equations are presented. Section III contains the results obtained for the correlation and response functions in a stationary driven state. We discuss our results in section IV, and conclude by considering some possible extensions of this work in section V.

II. DYNAMICAL EQUATIONS

A. The general framework

We start by briefly describing [12] the perturbative resummation schemes (of which the mode-coupling approximation is a special example) that allow to obtain closed equations for the time dependent correlation and response functions of an interacting system. We then specialize to the simpler case of a single mode, and study the resulting equations numerically.

Let us consider a system whose dynamics is described at the microscopic level by a Langevin equation

$$m \frac{\partial^2 \phi(\mathbf{x}, t)}{\partial t^2} + \frac{\partial \phi(\mathbf{x}, t)}{\partial t} = (-\mu(t) + \Delta) \phi(\mathbf{x}, t) - g \mathbf{F}(\phi) + \boldsymbol{\eta}(\mathbf{x}, t) + \mathbf{h}(\mathbf{x}, t), \quad (1)$$

where $\phi(\mathbf{x}, t)$ is a vector field, $\mathbf{F}(\phi)$ is a non-linear (possibly non-local) coupling term and $\boldsymbol{\eta}$ a Gaussian white noise. The term containing $\mu(t)$ is a restoring force and Δ may contain spatial derivatives or convolutions (as one would obtain for instance if ϕ is a coarse-grained density and the evolution is driven by the Ramakrishnan-Youssouf density functional, see e.g. [13]). The coupling constant g serves as a book-keeping parameter to set up a perturbative expansion.

Making a spatial Fourier transform, we obtain the fields $\hat{\phi}(\mathbf{k}, t)$ and the Gaussian noise such that $\langle \eta(\mathbf{k}, t) \eta(\mathbf{k}', t') \rangle = 2T \delta(\mathbf{k} + \mathbf{k}') \delta(t - t')$. In terms of those Fourier transformed variables, the correlation and response functions are defined as

$$\delta(\mathbf{k} + \mathbf{k}') C(\mathbf{k}, t, t') = \langle \hat{\phi}(\mathbf{k}, t) \hat{\phi}(\mathbf{k}', t') \rangle, \quad (2)$$

$$\delta(\mathbf{k} + \mathbf{k}') R(\mathbf{k}, t, t') = \left\langle \frac{\delta \hat{\phi}(\mathbf{k}, t)}{\delta \mathbf{h}(\mathbf{k}', t')} \right\rangle. \quad (3)$$

The dynamical equation (1) implies a Dyson equation for C and R of the form

$$m \frac{\partial^2 C(\mathbf{k}, t, t')}{\partial t^2} + \frac{\partial C(\mathbf{k}, t, t')}{\partial t} = (-\mu(t) \delta(\mathbf{k}') + \Delta_{\mathbf{k}'}) C(\mathbf{k} - \mathbf{k}', t, t') + 2TR(\mathbf{k}, t', t) \\ + \int_{-\infty}^{t'} dt'' D(\mathbf{k}', t, t'') R(\mathbf{k} - \mathbf{k}', t', t'') + \int_{-\infty}^t dt'' \Sigma(\mathbf{k}', t, t'') C(\mathbf{k} - \mathbf{k}', t'', t'), \quad (4)$$

$$m \frac{\partial^2 R(\mathbf{k}, t, t')}{\partial t^2} + \frac{\partial R(\mathbf{k}, t, t')}{\partial t} = (-\mu(t) \delta(\mathbf{k}') + \Delta_{\mathbf{k}'}) R(\mathbf{k} - \mathbf{k}', t, t') + \delta(t - t') \\ + \int_{t'}^t dt'' \Sigma(\mathbf{k}', t, t'') R(\mathbf{k} - \mathbf{k}', t'', t') \quad (5)$$

where the summation over \mathbf{k}' is implied. The operator $\Delta_{\mathbf{k}}$ acts now in the Fourier space. The functions $\Sigma(\mathbf{k}, t, t')$ and $D(\mathbf{k}, t, t')$ can be obtained [15] as *functionals* of the correlations and responses by adding all the two-line irreducible diagrams of the perturbative expansion in g of (1) but substituting the propagators with the dressed propagators $C(\mathbf{k}, t, t')$ and $R(\mathbf{k}, t, t')$. Now, if we stay at the level of the simplest diagrams (having only two vertices), we obtain the simplification¹ that $\Sigma(\mathbf{k}, t, t')$ and $D(\mathbf{k}, t, t')$ become ordinary *functions* of $C(\mathbf{k}, t, t')$ and $R(\mathbf{k}, t, t')$ (with no integrations over the times). This type of ansatz constitutes the basis of the mode-coupling approximation.

Naively, one could expect that the mode-coupling strategy could be improved to any desired accuracy by including diagrams with higher order vertices. Unfortunately, it seems that the phenomena usually described as “activated processes” are of a non-perturbative nature, and hence will be missed even if higher order vertices are taken into account. This is an intrinsic limitation of the mode-coupling or mean-field approaches when applied to realistic systems, and has to be taken into account when interpreting the results. We shall discuss this point in a more detailed way at the end of Section II D.

B. A single-mode driven model

Staying within this approximation, we furthermore make the considerable simplification of considering a single k -mode. This of course means that we give up all spatial information. The basic elements we find, however, can be readily generalized to the case of many k -modes, and, furthermore, to approximations that include diagrams with more and more vertices. The spirit is similar to the study of “schematic models” for the theory of supercooled liquids by Götze and coworkers [7]. These models are also closely related to spin glass ones, as explained in the next section. No attempt is made to describe in a *quantitative* way the rheology of glassy systems, but still it is hoped that *generic* and non-trivial behaviors can be predicted at a qualitative level.

If we restrict equation (5) to a single “important” mode, and furthermore absorb Δ which is now irrelevant in μ , and neglect the inertial term which is inessential for the slow dynamics, we obtain

$$\begin{aligned} \frac{\partial C(t, t')}{\partial t} &= -\mu(t)C(t, t') + 2TR(t', t) + \int_{-\infty}^{t'} dt'' D(C(t, t''))R(t', t'') + \int_{-\infty}^t dt'' \Sigma(t, t'')C(t'', t'), \\ \frac{\partial R(t, t')}{\partial t} &= -\mu(t)R(t, t') + \delta(t - t') + \int_{t'}^t dt'' \Sigma(t, t'')R(t'', t'). \end{aligned} \quad (6)$$

If in addition, we impose $C(t, t) = 1$ we have

$$\mu(t) = T + \int_{-\infty}^t dt'' [D(C(t, t''))R(t, t'') + \Sigma(t, t'')C(t, t'')]. \quad (7)$$

When the force in the Langevin equations derives from a potential, *so that detailed balance is verified*, one has [12]

$$\Sigma(t, t') = D'(C(t, t'))R(t, t'), \quad (8)$$

with $D'(x) \equiv dD(x)/dx$. Conversely, a set of equations with $\Sigma(t, t') - D'(C(t, t'))R(t, t') \neq 0$ can only describe a driven system, in which detailed balance is violated. Mode-coupling equations that describe a driven system can therefore be obtained by introducing a modified version of equation (8). Cugliandolo *et al* [16] chose for instance

$$\Sigma(t, t') = \alpha D'(C(t, t'))R(t, t'), \quad (9)$$

the parameter $1 - \alpha$ being then a measure of the (non-conservative) driving forces. They showed numerically that the presence of the drive was sufficient to stop aging in the glassy phase, so that time translation invariance was recovered at all temperatures.

¹This is a resummation and is not the same as expanding only to order g^2 , since the propagator themselves depend also on g .

It may be important at this point to distinguish between two ways of driving a system:

(i) “Shear-like” driving: the system is subjected to forces that do not derive from a global potential, as when a potential difference is applied at the ends of a conductor and the circuit is closed. They can be time-dependent or constant, and generate currents in both cases.

(ii) “Tapping-like” driving: the forces are time-dependent but do derive from a global potential. This is for example the case of an a.c. magnetic field in spin models, or oscillating acceleration of a container with frictionless walls (an a.c. gravity field). These forces do not do work if they are constant in time, independently of their strength.

In this paper we concentrate on the case of continuous drive, and hence only the “shearing-like” forces are relevant. We discuss below how the analogy with a rheological experiment can be developed further. The case of an oscillating drive will be discussed elsewhere.

C. The associated disordered model, and the rheological analogy.

Many years ago, Kraichnan [17] noted that one could find a disordered model such that the approximate closed equations for the two-point correlations and responses of the original model are *exact* for it. Although this hidden model behind the closure approximation is not otherwise directly related to the original one, it allows to view the dynamical equations from a different, instructive perspective.

We now specify the model we concentrate on in the rest of the paper. The case of the single mode equations with $D(x) = px^{p-1}/2$ corresponds to a disordered model given by continuous variables s_i ($i = 1, \dots, N$) evolving with the Langevin equation

$$\frac{\partial s_i(t)}{\partial t} = -\mu(t)s_i(t) - \frac{\delta H}{\delta s_i(t)} + f_i^{\text{drive}}(t) + \eta_i(t), \quad (10)$$

where

$$H = - \sum_{j_1 < \dots < j_p} J_{j_1 \dots j_p} s_{j_1} \dots s_{j_p} \quad (11)$$

is the Hamiltonian of the p -spin model and

$$f_i^{\text{drive}} = \epsilon(t) \sum_i^* \tilde{J}_i^{j_1 \dots j_{k-1}} s_{j_1} \dots s_{j_{k-1}}, \quad (12)$$

with $\sum_i^* \equiv \sum_{i < j_1 < \dots < j_{p-1}} + \sum_{j_1 < i < j_2 < \dots < j_{p-1}} + \dots + \sum_{j_1 < \dots < j_{p-1} < i}$. The parameter $\mu(t)$ ensures a spherical constraint $\sum_i s_i^2 = N$, and $\eta_i(t)$ ($i = 1, \dots, N$) are random Gaussian variables with mean 0 and variance $2T$. The couplings J in H are random Gaussian variables, symmetrical about the permutations of (j_1, \dots, j_p) , with mean zero and variance $p!/2N^{p-1}$. The couplings \tilde{J} in f_i^{drive} are random Gaussian variables, symmetrical about the permutations of (j_1, \dots, j_{k-1}) , with mean zero and such that

$$\overline{\tilde{J}_i^{j_1 \dots j_{k-1}} \tilde{J}_i^{j_1 \dots j_{k-1}}} = \frac{k!}{2N^{k-1}}; \quad \overline{\tilde{J}_i^{j_1 \dots j_{k-1}} \tilde{J}_{j_r}^{j_1 \dots i \dots j_{k-1}}} = 0. \quad (13)$$

The resulting force cannot be written as the derivative of a potential.

Equations (6) are then the exact equations satisfied by $C(t, t') = \sum_i \langle s_i(t) s_i(t') \rangle / N$ and $R(t, t') = \sum_i \langle \delta s_i(t) / \delta \eta_i(t') \rangle / N$ in the limit $N \rightarrow \infty$ and with $C(t, t)$ imposed. The model studied in Ref. [16] corresponds to $k = p$.

The important point is that, on average, *only the non-conservative part of the force gives energy to the system*, hence the name “driving force”. The amplitude of the drive is controlled by the parameter $\epsilon(t)$. If we now want to push further the analogy with the dynamics of a fluid system undergoing shear flow, we have to identify the equivalent of the shear rate and stress variables. Obviously, the schematic character of the model makes it difficult to carry out such an identification at a microscopic level. A way of bypassing this difficulty is to

estimate the power input into the system due to the existence of the non-conservative forces, which can be defined as

$$P \equiv \overline{\left\langle \frac{1}{N} \sum_{i=1}^N f_i^{\text{drive}} s_i \right\rangle}. \quad (14)$$

The calculation of this quantity is given in detail in the appendix, and assuming stationarity (see below) yields

$$P = \frac{k\epsilon^2}{2} \int_0^{+\infty} d\tau C(\tau)^{k-1} \frac{dR(\tau)}{d\tau}. \quad (15)$$

If we assume that the fluctuation dissipation theorem is not violated too strongly, as will be the case in the following examples, R is roughly proportional to dC/dt . Hence the power dissipated in the system will scale as ϵ^2/t_α , where t_α is the relaxation time of the system. Comparing to a standard shear flow, this indicates that ϵ should in that case be interpreted as playing the role of a stress, while ϵ/t_α is analogous to a shear rate.

Although equation (15) can be used to define the analogous of shear rate and shear stress in our model, the response function R does not have a direct analog in rheological measurements, since it is not the response associated to a shear stress. Experimentally, one should think of R and C as the response and correlation functions associated to an observable which is not rheologically relevant (as measured e.g. in a dielectric measurement). This observable would be measured in a system made stationary by imposing an external shear rate.

D. Reynolds effect and yield stress

Having access to a microscopic model behind the dynamical equations allows us to understand the evolution from the geometry of the corresponding phase-space. At zero external drive, this connection has been studied in much detail [18–21], and the main results can be summarized as follows.

At a given temperature, the free energy landscape of the purely conservative model with energy (11) can be constructed. Above a dynamical transition temperature T_c , the available phase space is dominated by one large basin in the free energy, corresponding to the paramagnetic (or “liquid”) state. At T_c , a *threshold level* in free energy appears, below which the free-energy surface is split into exponentially many disconnected regions.

The aging dynamics below T_c can be understood [22] as a gradual descent to the threshold level, starting from high energy configurations. The slowing down is then the consequence of the decreasing connectivity of the visited landscape. The system never really reaches the deeper, very disconnected parts of phase-space below the threshold. On the other hand, if the system is somehow prepared in one of these deep regions, it remains trapped there for all times.

When the system is quenched from a high temperature, but at the same time driven by non-conservative forces, it remains drifting above the free energy threshold, constantly receiving energy from the drive. In a mean-field system, such a situation will hold for arbitrarily weak drive, since the undriven system itself never falls below this energy level.

If, on the contrary the system is prepared in an energy state below the threshold, we expect that a weak driving force will have essentially no effect (beyond an “elastic” response of the system), as it is not strong enough to make the system overcome the barriers. If instead a strong drive is applied, the system escapes the low-lying valley and it surfaces above the threshold, where the drive will suffice to keep it forever (recall that in the rheological analogy, by “drive”, we really mean a stress). An interesting analogy can be drawn with the Reynolds dilatancy effect [4] in granular materials, or with the yield stress in a Bingham fluid [2]. Note that the actual value of valley depths and threshold level can be calculated from first principles within the same scheme of approximation we have used for the dynamics, starting from the original microscopic model.

We are now in a position to see what is the main shortcoming of the mode-coupling kind of approach. In any realistic system the structure of threshold and valleys may remain essentially the same, but now activated (non-perturbative) processes allow to jump barriers that are impenetrable at the perturbative level. Hence, for a real system the relaxation (aging) process will allow the system to penetrate slowly below the threshold, and after long times to access deeper valley. In order to keep the system with activated processes from sinking, we now need driving forces with finite strength (the “yield stress” effect). This effect can be expected to take place

whenever the system has fallen out of equilibrium, and is undergoing an aging process. Aging dynamics leads the system to be trapped (on the experimental time scale) in some deep lying valley. A strong enough drive can force to leave the valley, and a small extra drive is sufficient to keep the system above the threshold.

III. RESULTS FOR A STEADY DRIVE

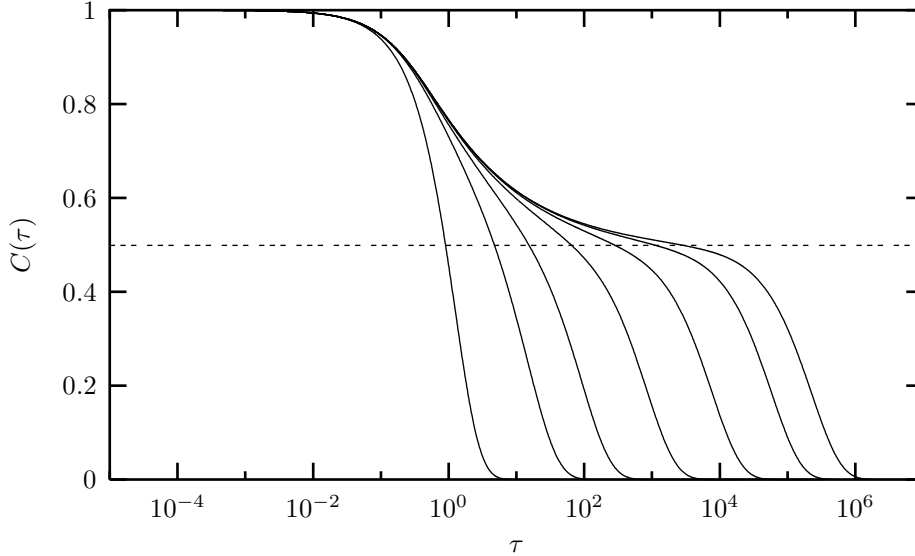


FIG. 1. Correlation function vs. time at $T = 0.613 > T_c$ for different driving forces. From left to right: $\epsilon = 5, 0.333, 0.143, 0.05, 0.0158, 0.00447$ and 0 . The longest plateau corresponds then to the undriven case.

A. Dynamical equations in the stationary state

When the system is submitted to a steady drive, it eventually reaches a stationary state, whatever the temperature. This allows to replace in equations (6) the two-times functions $A(t, t')$ by $A(\tau)$ with $\tau \equiv t - t'$. The following equations corresponding to the simple model described in section II C are easily obtained:

$$\begin{aligned}
 \frac{dC(\tau)}{d\tau} &= -\mu C(\tau) + \int_0^\tau d\tau' \Sigma(\tau - \tau') C(\tau') + \int_0^{+\infty} d\tau' [\Sigma(\tau + \tau') C(\tau') + D(\tau + \tau') R(\tau')], \\
 \frac{dR(\tau)}{d\tau} &= -\mu R(\tau) + \int_0^\tau d\tau' \Sigma(\tau - \tau') R(\tau'), \\
 \mu &= T + \int_0^{+\infty} d\tau' [D(\tau') R(\tau') + \Sigma(\tau') C(\tau')], \\
 D(\tau) &= \frac{p}{2} C(\tau)^{p-1} + \epsilon^2 \frac{k}{2} C(\tau)^{k-1}, \\
 \Sigma(\tau) &= \frac{p(p-1)}{2} C(\tau)^{p-2} R(\tau).
 \end{aligned} \tag{16}$$

Note that these equations are “non-causal” in the time difference τ . They are of course still causal in the original two times, but the parity of $C(\tau)$ has now been used.

The system (16) can only be solved analytically in the limit of small drive, for all temperatures, following the steps of Ref. [22]. The solution shows that the correlation and response functions can be split into two parts associated with the two time scales discussed in the introduction. One then writes $C(\tau) = C_s(\tau) + C_f(\tau)$ and

$R(\tau) = R_s(\tau) + R_f(\tau)$, ‘ f ’ (‘ s ’) labeling the ‘fast’ (‘slow’) time-scale. In that small drive limit, the two time scales are well separated and the fluctuation-dissipation theorem (FDT) does not hold. More precisely, one can prove a generalization of the FDT, in the form

$$R_f(\tau) = -\frac{1}{T} \frac{dC_f(\tau)}{d\tau}; \quad R_s(\tau) = -\frac{1}{T_{\text{eff}}} \frac{dC_s(\tau)}{d\tau}. \quad (17)$$

An interpretation is that the short time scale is thermalized at the bath temperature T , while the longer one is thermalized at an effective temperature T_{eff} [1]. This effective temperature is determined analytically by the matching of the solutions between the two time scales. It is interesting to remark that the values of the effective temperatures for a stationary, very weakly driven system coincides with the effective temperature of its undriven, aging counterpart.

In order to study the pre-asymptotic ($\epsilon \neq 0$) behavior of the system, we solved numerically the system (16), combining the numerical methods of Refs. [23,24]. In the next section, we discuss the numerical results obtained for the case $k = p = 3$. The cases $k = 2$, $p = 3$ and $k = p = 4$ have also been studied numerically, with very similar results. We discuss in two different subsections the results for $T > T_c$ and $T < T_c$.

B. Above the glass transition temperature, $T > T_c$

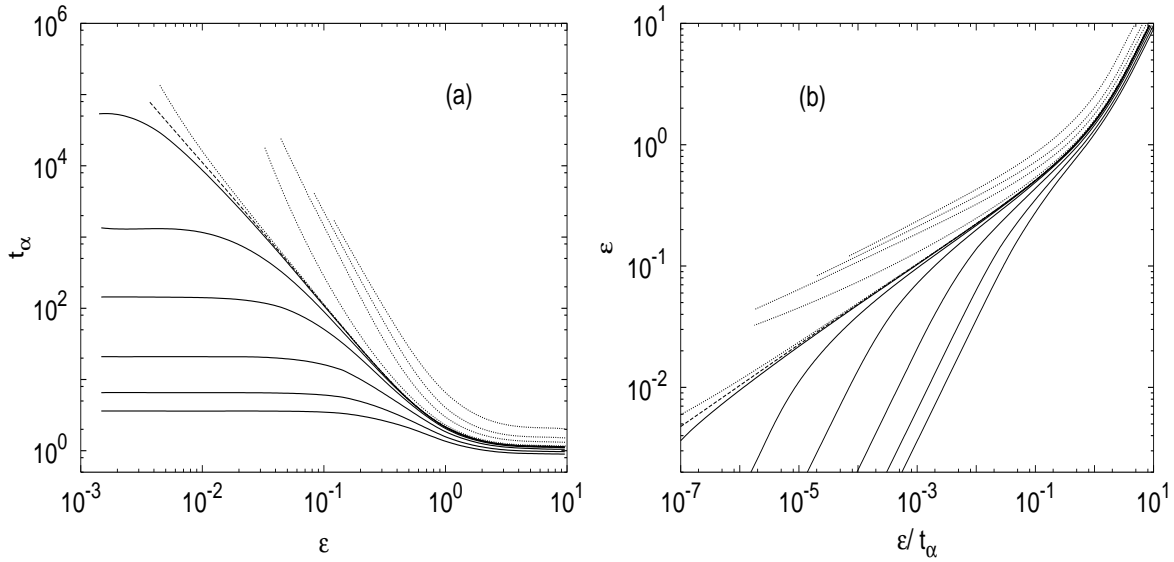


FIG. 2. (a) Alpha-relaxation time as a function of drive for temperatures (from bottom to top) $T = 0.9, 0.8, 0.7, 0.64, 0.62, 0.613, T_c \simeq 0.61237, 0.6115, 0.58, 0.45, 0.3, 0.01$. Full lines are for temperatures above T_c , the dashed line is $T = T_c$, and the dotted lines are for $T < T_c$. (b) Flow curves analogous to the usual σ vs $\dot{\gamma}$ for the same temperatures in the same order.

The correlation function decay above the glass transition temperature is a two-step process, as shown in figure 1. The length of the plateau (the α -relaxation time t_α) increases as the glass transition temperature is approached. At fixed temperature, for stronger driving forces the plateau region becomes shorter, and for a sufficiently strong drive the process has no longer two distinct time scales. In what follows, we focus on the not too strong drive regime in which two steps are still discernible.

The full lines in figure 2-a show the variations of t_α as a function of the amplitude of the driving force ϵ above T_c . The relaxation time is defined here as $t_\alpha(\epsilon, T) \equiv \int_0^{+\infty} d\tau C(\tau)$. In the rheological analogy, t_α is expected to play the role of a viscosity (which, generally speaking, scales as the structural relaxation time). Hence these curves are somewhat analogous to the ‘‘flow curves’’ measured in non-Newtonian fluids, and they give the behavior of the viscosity as a function of the shear stress. The translation to the more common plot σ (for us ϵ) as a function of $\dot{\gamma}$ (for us ϵ/t_α) is done in figure 2-b.

Above the glass transition ($T > T_c$), t_α levels off at a finite value $t_0(T)$ when the drive vanishes, except at exactly T_c where it diverges like $\epsilon^{-\beta}$ (the value of β is discussed below). The Mode-Coupling Theory [7] gives the scaling of t_0 when approaching T_c and, for the model studied here, implies $t_0(T) \sim (T - T_c)^{-1.765}$, which is very well verified numerically. Above T_c , the curves of figure 2-a exhibit a plateau for small driving forces whose height diverges as $T \rightarrow T_c$. This plateau corresponds to a Newtonian regime in the language of rheology, sometimes also called “linear regime”. By this we mean that the relaxation time in this region (small values of ϵ) is essentially independent of the drive, implying that the drive does not substantially alter the dynamics of the system.

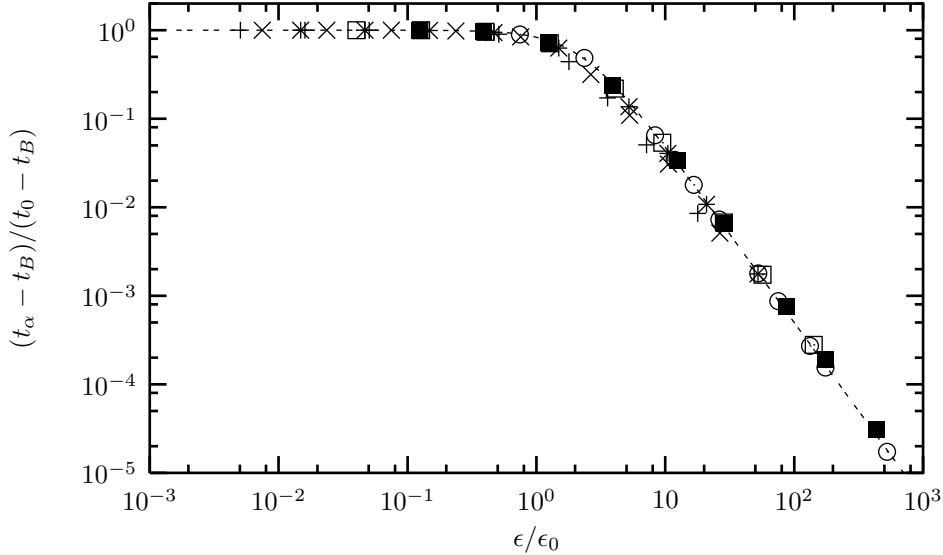


FIG. 3. Scaling plot of t_α versus drive for several temperatures above the transition $T = 0.9, 0.8, 0.7, 0.64, 0.62$ and 0.613 . The dashed line is the fit $1/(1+x^2)$.

For stronger driving forces, the relaxation time decreases, a *shear thinning* effect. The expression

$$t_\alpha(\epsilon, T) = t_B + \frac{t_0 - t_B}{1 + \left(\frac{\epsilon}{\epsilon_0}\right)^\beta} \quad (18)$$

fits the relation $t_\alpha(\epsilon, T > T_c)$ very well as can be seen in figure 3. The fit is obtained (following Ref. [25]), by defining $t_B(T) \equiv \lim_{\epsilon \rightarrow \infty} t_\alpha$, and the second fitting parameter ϵ_0 as $t_\alpha(\epsilon_0) \equiv 0.8t_0$. Numerically, we find $\beta = 2$. Interestingly, the same β is found for the other cases (corresponding to $k = 2, p = 3$ and $k = p = 4$) we have considered. We note that such an exponent is clearly non-trivial, in the sense that it could not be predicted from a simple dimensional argument.

The shear thinning effect is well documented in systems as different as gels, polymers or supercooled liquids [2,3,25,26], and shear thinning curves are known to be well represented by expressions similar to equation (18). It is then tempting to interpret our results in terms of shear rate and stress, using the analogy developed at the end of section II C. It is easily seen that for high “shear rates” (defined as $\dot{\gamma} \equiv \epsilon/t_\alpha$, equation (18) with $\beta = 2$ implies the relation $t_\alpha \sim \dot{\gamma}^{-2/3}$. Remarkably, this is very similar to the shear thinning relationship observed in polymeric systems (for other systems a variety of similar relationships can be observed, with shear thinning exponents that are usually between $-1/2$ and -1).

Note finally that at very strong drive, the relaxation time becomes of the order of the microscopic time ($t_B \sim 1$ in reduced units and depends only slightly on temperature), the system being Newtonian again.

We now turn to the study of the fluctuation dissipation relation in the driven system. In the absence of drive, the FDT holds for $T > T_c$. Hence a plot of the integrated response $\chi(\tau) \equiv \int_0^\tau R(\tau')d\tau'$ as a function of C gives a straight line with slope $-1/T$. In figure 4 we show such a plot for several strengths of the drive ϵ . We immediately note that the χ vs. C curve is, for non-zero drive, well approximated by a broken line, with a first

piece having a slope $-1/T$ (corresponding to the fast relaxation) and a second piece that displays a smaller slope, denoted in the following by $-1/T_{\text{eff}}$ by analogy with the analytical results of the above section.

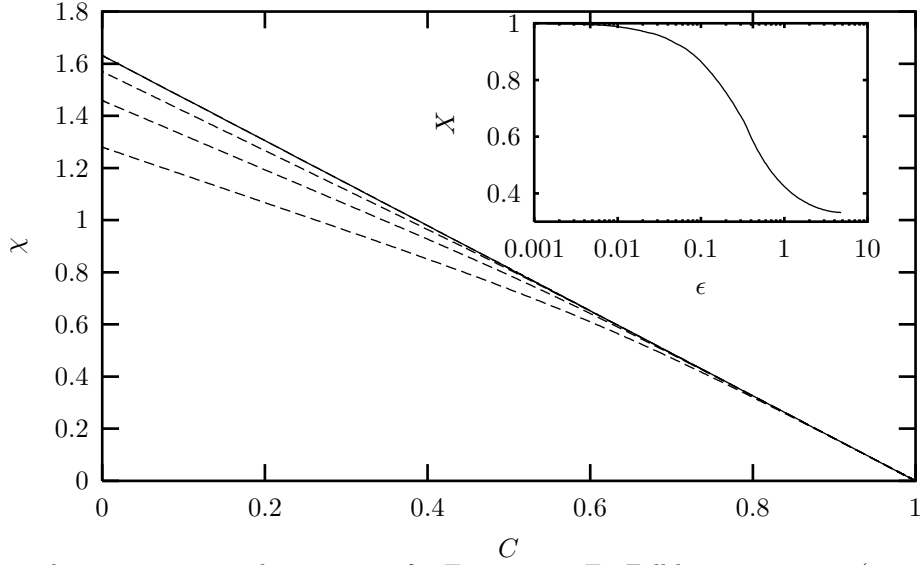


FIG. 4. Integrated response vs. correlation curves for $T = 0.613 > T_c$. Full line: asymptotic ($\epsilon = 0$) analytical curve. Dashed lines (from bottom to top) $\epsilon = 0.333, 0.143, 0.05, 0$. Inset: behavior of the FDR as a function of the drive ϵ for $T = 0.613$.

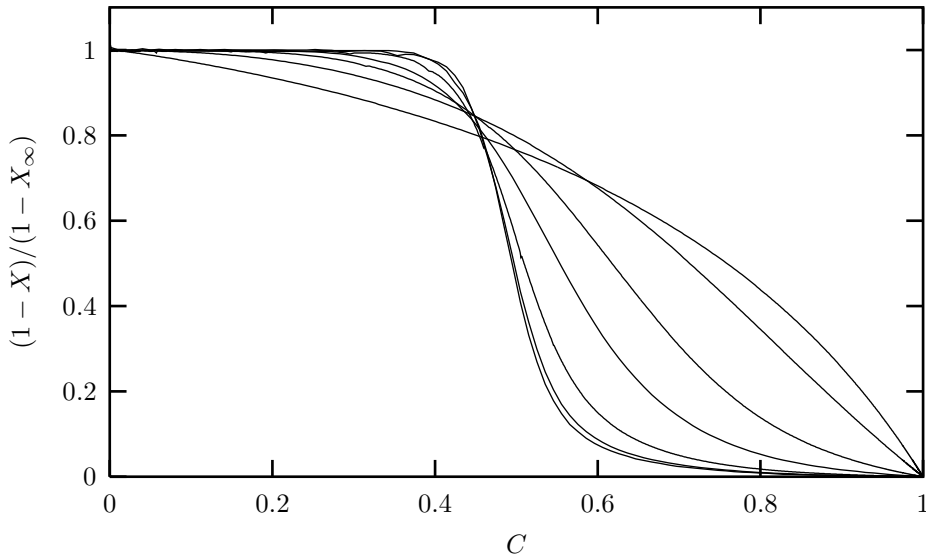


FIG. 5. Normalized fluctuation-dissipation ratio X versus the correlation C for $\epsilon = 0.00141, 0.0141, 0.0448, 0.143, 0.333, 1, 5$ (from bottom to top at $C = 0.8$). The temperature is $T = 0.62$.

To make the assumption of a “two-temperature regime” very clear, we plot in Figure 5 the normalized

fluctuation-dissipation ratio (FDR)

$$X \equiv \frac{TR(\tau)}{dC(\tau)/d\tau} \quad (19)$$

(the normalized derivative of the curves 4) for several values of the drive. The numerical solution shows clearly that, although the effective temperature T_{eff} is unambiguously defined only in the asymptotic limit ($T \rightarrow T_c, \epsilon \rightarrow 0$), the “two straight lines” approximation is very good even at finite driving forces and of course improves as $\epsilon \rightarrow 0$.

The violation of the FDT in a driven system is an important concept, since it quantifies the deviation from the Boltzmann weight in the phase space distribution of the system. The inset of figure 4 shows how the ratio $X = T_{\text{eff}}/T$ that characterizes this violation changes with the driving force. For small drives, the deviation from one is very small, which allows to define a zone in the plane (ϵ, T) where the “linear response” (in the sense of irreversible thermodynamic theory) holds. This zone happens to coincide with the “linear regime” defined from the rheological point of view. This suggests that there is a direct link between a non-linear response in rheological measurements and a non-equilibrium behavior from the statistical mechanics point of view. Note also that one still might study the linear rheology (typically the behavior of $G^*(\omega)$) of an aging (and hence out of equilibrium) system, see [27].

C. Below the glass transition temperature, $T < T_c$

Below T_c , an undriven system never equilibrates, the α -relaxation time grows with the waiting time elapsed after the quench into the glassy phase, and the system never becomes stationary. If we now quench the system with driving forces acting on it, it turns out that the α -relaxation time becomes finite, and the system eventually becomes stationary [4,9,10]. For vanishingly small drive, however, t_α will again diverge. The dotted lines in figure 2-a show this divergence of t_α with decreasing drive. For temperatures just below T_c , the times at first diverge like ϵ^{-2} : the same regime was already noted above T_c . Still decreasing ϵ , they then cross over to another, faster divergence. Numerically, we find that $t_\alpha(\epsilon \ll 1, T < T_c) \sim \epsilon^{-\alpha(T)}$, with $\alpha(T)$ slowly (if at all) dependent on temperature. For instance, at $T = 0.3$, we obtain $\alpha \simeq 3.19$. To summarize, below T_c , the system does not have a “Newtonian” or linear response region, and exhibits shear thinning $t_\alpha \sim \epsilon^{-\alpha}$. This power law divergence is also found numerically and in a rather involved analytical treatment by Horner in the case of the forced particle in a random potential, where it is called a “creep” behavior [10].

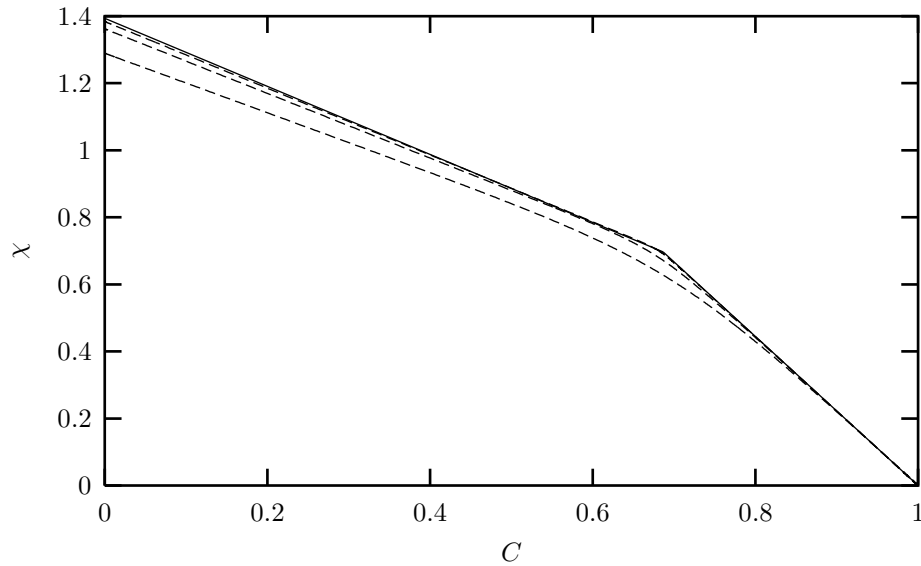


FIG. 6. Integrated response vs. correlation curves for $T = 0.45 < T_c$. Full line: asymptotic ($\epsilon = 0$) analytical curve. Dashed lines (from bottom to top) $\epsilon = 0.333, 0.143, 0.0442$.

Turning now to FDT, the situation is quite different from the one at $T > T_c$ (figure 6). The “two-temperature scenario” persists even for vanishingly small drives, giving a clear demonstration of the difference between a glass driven to stationarity and an equilibrium system. It is very reminiscent of what happens in the aging (undriven) situation: we already noted that the limiting effective temperatures were the same in both situations.

IV. DISCUSSION: THE TEMPERATURE-DRIVE “PHASE DIAGRAM”

A convenient synthetic representation of the main results obtained in this paper is given in figure 7, which represents a “phase diagram” of the system in the plane (ϵ, T) . In such a two dimensional representation, the usual glass phase is restricted to the segment $T < T_c$ of the horizontal axis. Other points in the plane corresponds to states which respect time translation invariance, and can be characterized by their relaxation time t_α and their fluctuation dissipation ratio. The two families of curves drawn in figure 7 correspond indeed to constant values of t_α (“iso- t_α ”) and constant values of the long-time FDR (“iso- X ”). From these curves, it is manifest that when the drive is taken into account, the influence of the glassy phase extends far beyond the horizontal axis, in the sense that systems with values of X characteristic of the glass are found at high temperatures for finite drives. The effect of shear is in a sense paradoxical, because at the same time it makes a glass “liquid-like” (by fluidifying it), and it brings about typical glass features (two temperatures) to a supercooled liquid which otherwise would be at equilibrium.

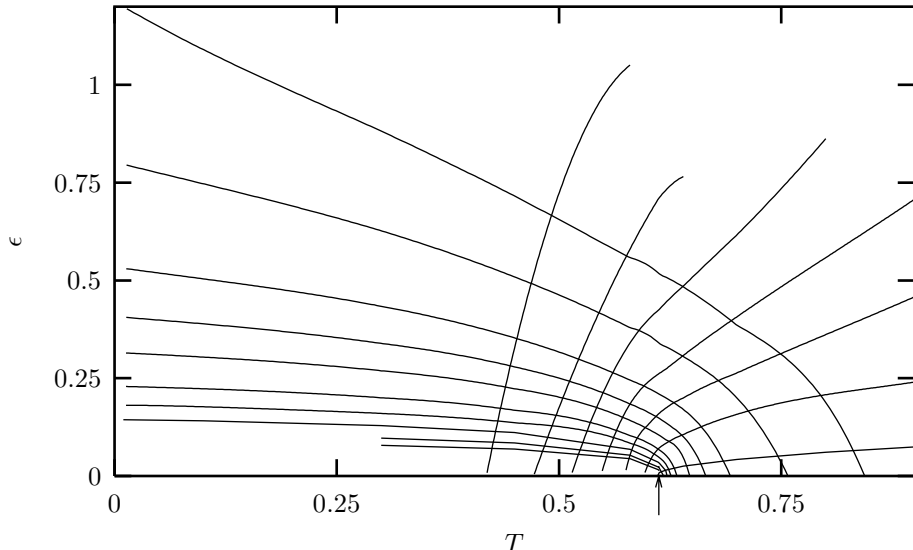


FIG. 7. 2D view of the glass transition. Curves bent to the left are the iso- t_α , curves bent to the right are the iso- X (see text). The critical temperature is indicated by the arrow. Times are $t_\alpha = 5, 10, 25, 50, \dots, 5000$ (from top to bottom), and $X = 0.4, 0.5, 0.6, 0.7, 0.8, 0.9, 0.99$ (from left to right).

Our two dimensional phase diagram is obviously closely related to the (Load, Temperature) phase diagram proposed by Liu and Nagel in an attempt to rationalize the similarities in behavior between glasses and granular matter [28]. In practice, the glass transition temperature is defined as the temperature where the viscosity (or relaxation time) exceeds a predefined threshold. Hence the surface drawn by Liu and Nagel to delimit “jammed” (or glassy) and “unjammed” (or liquid) states would correspond in our graph to an iso- t_α line.

The “near equilibrium” region of our phase diagram can be defined for example as the zone where $X > 0.99$ (note the initially flat behavior of $X(\epsilon)$ in the inset of figure 4). In this region, the usual near-equilibrium concepts are applicable. As the glass transition is approached, this region becomes restricted to weaker and weaker driving forces, and the two-temperature behavior typical of the glassy phase is observed. In the further limit of very large (probably unphysical in many cases) driving strengths, when the relaxation time scale becomes of the order of the microscopic time, the concept of T_{eff} becomes of course badly defined.

As mentioned above, the prediction of a sharp, purely dynamic glass transition is an unrealistic feature of any theory not taking into account activated processes. It seems healthy at this point to discuss in some detail what kind of new features are to be expected in real situations, when the effect of activated processes is present. In figure 8 we sketch the modifications that can be expected in a realistic system in which the dynamic transition is smeared by activated processes. To begin with, at zero drive there is a finite equilibration time at all temperatures above T_k ($T_k < T_c$), the (so-defined) Kauzmann temperature, which may or may not be zero. Given a system above T_k there will, in principle, always be a sufficiently small driving force such that FDT still holds. However, not all of the drive-temperature plane is accessible in stationary (non-aging) conditions. Given an experimental situation, there is a level (the thick line in Fig. 8) below which the system does not have the time to become stationary. this is the “glass transition” (in fact, a crossover) as it happens in practice, and the zero-drive intercept of this line is usually denoted the “glass transition temperature” T_g .

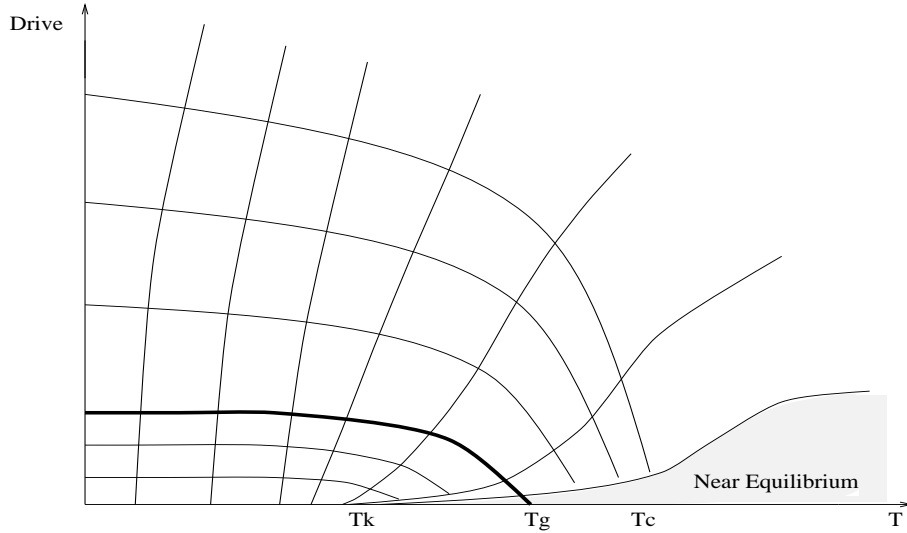


FIG. 8. Same as figure 7, but with the activated processes taken into account (schematic).

From what we have learned from the idealized case, we might expect that above T_g , in conditions such that the α -relaxation time and therefore the viscosity are already large, there will be a well established two-temperature regime as soon as a moderately weak driving is turned on. The consequence is that in the supercooled liquid regime for instance, a small shear rate will be sufficient to give at the same time a non-linear rheological behavior (as seen in the MD simulations of reference [3]), and an *effective temperature different from that of the thermostat*. Such an effect would also be accessible in an experiment. We stress that an effective temperature could be measured in that case *in a stationary state* making the measurements far easier than in an aging experiment [29].

Below the “glass transition” line, on the contrary, we expect that, as discussed in section IID, history dependent effects will become predominant, with effects like yield stress or hysteresis that cannot be accounted for within mean-field like theoretical schemes.

Having pointed out all these differences, the basic suggestion of a two steps, two temperatures relaxation behavior remains, and is open for numerical and experimental checks.

V. CONCLUSIONS AND PERSPECTIVES

In this paper, we have studied, within the framework of the mean-field (or mode-coupling) approximation, the influence of an external drive on a system undergoing a glass transition. The main results of the approach should, we believe, not depend too strongly on the method of approximation. Hence we have constantly tried to interpret the results within the context of a rheological experiment on a system with anomalous rheology, although such an interpretation remains of course rather tentative.

In this language, we can summarize our results as follows. If a fluid having, in equilibrium, two well-separated relaxation time scales is gently driven (e.g. sheared) the slow structural relaxations are accelerated (shear thinning). This acceleration is accompanied by the appearance of an effective temperature for the slow structural degrees of freedom, while the fast degrees of freedom (phonons, etc) are still at the bath temperature. Each temperature is associated with fluctuations at each time scale, and is well-defined if the drive is gentle enough that the time scales still remain separated [30]. When the two temperatures differ very little, “near equilibrium” assumptions becomes justified: this regime was shown to coincide with the usual “linear regime” of steady-state rheology. For stronger drive, a power law decay of the relaxation time with increasing drive is observed, as is the case in many complex fluids. Interestingly, the associated “shear thinning” exponent is found to be $-2/3$, and seems to be quite robust with respect to variations in the model. This could be an indication of why so many shear thinning exponents in real systems are found in the range $[-1/2, -1]$.

The obvious weakness of the approach, which is intrinsic to the perturbative scheme adopted, is that the effect of activated processes can only be described at a qualitative level. Hence a number of interesting phenomena observed at weak driving forces (e.g. yield stress, dilatancy, hysteresis) cannot be addressed analytically.

In principle, the present study could be extended to equations with many coupled spatial modes. One can even go further and consider richer resummation schemes, like for example the self consistent screening approximation [12]. Moreover, other resummations like applying to the driven case a dynamical version of the hypernetted-chain equation (in the spirit of the work on glasses of Mézard and Parisi [31]) can be envisaged. In this way, one could study a true shear applied to the largest spatial mode, and calculate how the energy cascades to the shorter wavelengths. The two-temperature ansatz can be shown to close [14] independently of the resummation scheme, with the important property that there are still in the small drive limit only two temperatures shared by all spatial modes. The implementation of these improvements may then allow to extract actual numbers starting from a realistic microscopic theory. However, it should be born in mind the non-perturbative activated processes would still remain inaccessible to these more sophisticated computational schemes.

ACKNOWLEDGMENTS

The numerical calculations presented in this work were carried out at the PSMN of ENS-LYON. We thank Arnulf Latz for providing us with a copy of the program described in Reference [24], and F. Thalmann for discussions. J. K. was partially supported by the “Programme Thématique Matériaux, Région Rhône-Alpes”.

APPENDIX: CALCULATION OF THE POWER INPUT

The quantity to estimate is

$$P \equiv \overline{\left\langle \frac{1}{N} \sum_{i=1}^N f_i^{\text{drive}} \dot{s}_i \right\rangle}. \quad (20)$$

To compute this quantity, we introduce a current h , and a generating functional Z such that

$$Z \equiv \overline{\left\langle \exp \left(\int dt \sum_i h_i(t) f_i^{\text{drive}} \dot{s}_i \right) \right\rangle}. \quad (21)$$

Then by definition

$$P(t) = \frac{1}{N} \sum_{i=1}^N \left[\frac{\delta Z}{\delta h_i(t)} \right]_{h=0}. \quad (22)$$

Z can be obtained from the usual Martin-Siggia-Rose (MSR) formalism, and the average over the random variables \tilde{J} gives the extra-term

$$\frac{k\epsilon^2}{4N^{k-1}} \sum_{i, j_1, \dots, j_{k-1}} \int dt dt' [s_{j_1}(t) s_{j_1}(t') \cdots s_{j_{k-1}}(t) s_{j_{k-1}}(t')] \times [i\dot{s}_i(t) i\dot{s}_i(t') + h_i(t) \dot{s}_i(t) h_i(t') \dot{s}_i(t') + 2i\dot{s}_i(t') h_i(t) \dot{s}_i(t)] \quad (23)$$

in the effective MSR Lagrangian. Finally, we obtain for P :

$$P(t) = \int \mathcal{D}s \mathcal{D}\hat{s} \exp(L) \frac{k\epsilon^2}{4N^k} \sum_{i,j_1,\dots,j_{k-1}} \int dt' [s_{j_1}(t) s_{j_1}(t') \cdots s_{j_{k-1}}(t) s_{j_{k-1}}(t')] [2i\hat{s}_i(t') \dot{s}_i(t)], \quad (24)$$

where L is the usual MSR Lagrangian for the p -spin model. The integral is estimated at its saddle point, yielding,

$$P(t) = \frac{k\epsilon^2}{2} \int_{-\infty}^t dt' C(t, t')^{k-1} \frac{\partial R(t, t')}{\partial t}. \quad (25)$$

which reduces for time translation invariant systems to

$$P = \frac{k\epsilon^2}{2} \int_0^{+\infty} d\tau C(\tau)^{k-1} \frac{dR(\tau)}{d\tau}. \quad (26)$$

- [1] L.F. Cugliandolo, J. Kurchan and L. Peliti, Phys. Rev. E **55**, 3898 (1997).
- [2] R.G. Larson, *The Structure and Rheology of Complex Fluids* (Oxford University Press, New York, 1999).
- [3] R. Yamamoto and A. Onuki, Europhys. Lett. **40**, 61 (1997); R. Yamamoto and A. Onuki, Phys. Rev. E **58**, 3515 (1998).
- [4] J. Kurchan, *Rheology, or how to stop aging*, preprint cond-mat/9812347.
- [5] J.-P. Bouchaud, L.F. Cugliandolo, J. Kurchan and M. Mézard in *Spin Glasses and Random Fields*, Ed.: A.P. Young (World Scientific, Singapore, 1998); preprint cond-mat/9511042.
- [6] P. Sollich, F. Lequeux, P. Hébraud and M.E. Cates, Phys. Rev. Lett. **78**, 2020 (1997); P. Sollich, Phys. Rev. E **58**, 738 (1998).
- [7] W. Götze, in *Liquids, Freezing and Glass Transition*, Eds.: J.P. Hansen, D. Levesque and J. Zinn-Justin, Les Houches 1989, (North Holland, Amsterdam, 1991); W. Götze and L. Sjögren, Rep. Prog. Phys. **55**, 241 (1992); W. Götze, J. Phys. Condens. Matter **11**, A1 (1999); W. Kob, p. 28 in *Experimental and Theoretical Approaches to Supercooled Liquids: Advances and Novel Applications*, Eds.: J. Fourkas, D. Kivelson, U. Mohanty, and K. Nelson (ACS Books, Washington, 1997).
- [8] J. A. Hertz, G. Grinstein and S. Solla in *Proceedings of the Heidelberg Colloquium on Glassy Dynamics and Optimization, 1986*, Eds: J. L. van Hemmen, I. Morgernstern, (Berlin, Springer Verlag, 1987); G. Parisi, J. Phys. A **19**, L675 (1986).
- [9] A. Crisanti and H. Sompolinsky; Phys. Rev. **A36**, 4922 (1987).
- [10] H. Horner, Z. Physik B **100**, 243 (1996).
- [11] F. Thalmann, Thesis University of Grenoble (1998); F. Thalmann, Eur. Phys. J. B **3** 497 (1998).
- [12] J.P. Bouchaud, L.F. Cugliandolo, J. Kurchan and M. Mézard, Physica A **226**, 243 (1996).
- [13] L.M. Lust, O.T. Valls and C. Dasgupta, Phys. Rev. E **48**, 1787 (1993).
- [14] L. F. Cugliandolo and J. Kurchan, Physica **A 263** (1999) 242.
- [15] C. de Dominicis and P.C. Martin, J. Math. Phys. **5** (1964) 14 and 31.
- [16] L.F. Cugliandolo, J. Kurchan, P. Le Doussal and L. Peliti, Phys. Rev. Lett. **78**, 350 (1997).
- [17] R. Kraichnan, J. Fluid Mech. **7**, 124 (1961).
- [18] J. Kurchan, G. Parisi and M.A. Virasoro, J. Phys. I France **3**, 1819 (1993).
- [19] A. Crisanti and H.J. Sommers, J. Phys. I France **5**, 805 (1995).
- [20] A. Cavagna, I. Giardina and G. Parisi, Phys. Rev. B **57**, 11251 (1998).
- [21] A. Barrat, R. Burioni and M. Mézard, J. Phys. A **29**, L81 (1996).
- [22] L.F. Cugliandolo and J. Kurchan, Phys. Rev. Lett. **71**, 173 (1993).
- [23] K. Ng, J. Chem. Phys. **61**, 2680 (1974).
- [24] M. Fuchs, W. Götze, I. Hofacker and A. Latz, J. Phys.: Condens. Matter **3**, 5047 (1991).
- [25] J.D. Ferry, *Viscoelasticity properties of polymers* (Wiley, New York, 1980).
- [26] R. Yamamoto and A. Onuki, *Rheology of a supercooled polymer melt*, preprint cond-mat/9906325; R. Khare, J. de Pablo and A. Yethiraj, J. Chem. Phys. **107**, 6956 (1997); A.V. Lyulin, D.B. Adolf and G.R. Davies, J. Chem. Phys. **111**, 758 (1999).

- [27] S. M. Fielding, P. Sollich and M. E. Cates, *Ageing and Rheology in Soft Materials*, preprint cond-mat/9907101.
- [28] A.J. Liu and S.R. Nagel, *Nature* **396**, 21 (1998).
- [29] T.S. Grigera and N. E. Israeloff, *Phys. Rev. Lett.* **83**, 5038 (1999).
- [30] The hopping temperature that plays an important role of in the SGR model [6] is more like the effective temperature of the slow modes here. It is not unlikely that a precise connection will be possible.
- [31] M. Mézard and G. Parisi, *J. Chem. Phys.* **111**, 1076 (1999).